IEEE Access
Multidisciplinary ⋮ Rapid Review ⋮ Open Access Journal

Received June 17, 2020, accepted June 29, 2020, date of publication July 8, 2020, date of current version July 20, 2020.

Digital Object Identifier 10.1109/ACCESS.2020.3007873

A Novel Method for Measuring Subtle Alterations in Pupil Size in Children With Congenital Strabismus

MARTÍN GALLEGOS-DUARTE[1], JORGE DOMINGO MENDIOLA-SANTIBAÑEZ[2], (Member, IEEE), DANJELA IBRAHIMI[1,2], CARLOS PAREDES-ORTA[3], JUVENAL RODRÍGUEZ-RESÉNDIZ[2], (Senior Member, IEEE), AND CARLOS ALBERTO GONZÁLEZ-GUTIÉRREZ[4]

[1]Facultad de Medicina, Universidad Autónoma de Querétaro, Santiago de Querétaro 76176, México
[2]Facultad de Ingeniería, Universidad Autónoma de Querétaro, Santiago de Querétaro 76010, México
[3]Centro de Investigaciones en Óptica, Unidad de Aguascalientes, Aguascalientes 20200, México
[4]Universidad del Valle de México Campus Querétaro, Santiago de Querétaro76230, México

Corresponding author: Jorge Domingo Mendiola-Santibañez (mendijor@uaq.mx)

This work was supported by UAQ, CONACyT, and PRODEP for the support with the laboratory, scholarship, and financial resources of this research.

ABSTRACT This paper analyzes a cohort of children diagnosed with congenital strabismus independent of the deviation direction, dissociated and non-dissociated, to identify anisocoria magnitude under scotopic conditions. This disease presents changes in the white matter affecting the nerve conduction in the cortical integrator, exacerbating the reflexes controlling pupil size, producing subtle changes in the pupil dimensions that are difficult to measure using current methods. The proposed indexes estimate the degree of anisocoria using the Feret diameter and the Pattern Pupil parameter. This research presents a prospective, transversal, and experimental study carried out on 168-Mexican children aged 5-15 years from Querétaro, México, diagnosed with dissociated and non-dissociated congenital strabismus. The utilized images come from videos of each patient recorded in scotopic lighting conditions (0.3 lux). The ophthalmologist measured the Feret diameters of both pupils using the ImageJ software. 11.9% of the sample group showed ''Very significant,'' and ''Significant'' degrees of anisocoria, whereas 88.1% of the sample group had ''Non-significant,'' and ''Few significant'' degrees of anisocoria. When comparing the results with those obtained using the perimeter, and the diameter, subtle variations of anisocoria were better detected using the area criterion. ANOVA experiments allowed the following: 1) dissociated and non-dissociated congenital strabismus identification using nidp index, and 2) the comparison of the anisocoria degrees identified by the nidp and Ddmm $\geq$ 0.4 mm indexes.

INDEX TERMS Anisocoria, anisocoria indexes, Feret diameter, pupil pattern, congenital strabismus.

I. INTRODUCTION

The neurophysiological balance between the dilator and constrictor muscles, the entrance of light, and the sympathetic and parasympathetic activity determine the size and shape of pupils [1], [2]. However, neurophysiological equilibrium may not be the same for both pupils, causing asymmetry in size or shape, or both and may also affect reaction speed [3]. When the difference in the diameter size of pupils is more than 0.4 mm, it is called anisocoria [4]–[6]. Experts usually check for anisocoria exploration under mesopic illumination, that is, with dim but not quite dark lighting. However, in some cases, researchers carry out the pupil measurements in scotopic lighting conditions, i.e., under very low-light levels almost in the dark, in which the small size of the pupil is considered pathological [7], [8]. Particularly in congenital strabismus, the exacerbation of the constrictor reflex appears only in scotopic conditions [9]. There are few reports on normative data concerning pupil size and anisocoria. Often, authors compare the diameter difference between a normal and a pathological pupil. If the difference is at least 0.4 mm, then this classifies as anisocoria. Nevertheless, there is no standard diameter difference obtained formally in research to identify anisocoria. Regardless of this situation, anisocoria indicates alterations in the structure of the pupillary function [5]; it serves as a sign to identify neurological state of the patient,

The associate editor coordinating the review of this manuscript and approving it for publication was Mohamad Forouzanfar.

and aids in medical making decisions. Therefore accuracy in identifying and measuring anisocoria is necessary [10]. Specialists have employed different methods to acquire the diameters of pupils. For example, they have used infrared photography and equipment to digitize with sufficient sensitivity to identify variations of 0.1 to 0.5 mm [11], [12].

On the other hand, traditional studies on anisocoria consider the perimeter or diameter and not the area of pupils [7], [13]. Because congenital strabismus is a disease with subtle neurological alterations, this model has been used to measure pupil asymmetry [14], [15]. Anisocoria is more evident for some neurological illnesses, and the specialist can measure it using an automated pupillometer. However, congenital strabismus is a biological model that offers subtle and gradual changes in pupil size. Hence these variations in dimensions are difficult to detect using the perimeter, and the diameter. To overcome this limitation, we introduced the concept of Pattern Pupil (PP) and we took the area of both pupils as key measurements.

Section II-C1 presents the PP concept using the average area computed from both pupils. As a consequence, small changes in their sizes are better detected. Therefore, the PP parameter permits the introduction of a reference to analyze each pupil independently using normalized indexes, and due to this characteristic, scale problems on the processed images do not appear. On the other side, the maximum Feret diameter of pupils allows computing a representative mean area. Section II-C2 presents a new index nidp, considering the arithmetic difference of the indexes iipr (for the right pupil) and iipl (for the left pupil) estimated individually. The new index nidp shows the presence of several degrees of anisocoria, indicating more sensitivity. The processed data graphically illustrate this behavior. Historically, in neuroimaging, a more accurate diagnosis prognostic appears with the use of more sensitive equipment [16], which can measure or detect small values. These medical instruments help the physician to get a better assessment [17] and correlate the new values with the clinic [18]. Thus the proposal of this paper agrees with this idea. In section II-C3, the computed indexes based on the perimeter, and diameter, are compared with the results found using the PP. Section III corresponds to the results and presents two studies of ANOVA. The first study shows that the subtle changes detected by the nidp index help to identify the dissociated and non-dissociated congenital strabismus, and the other analysis compares the different degrees of anisocoria recognized with the nidp and Ddmm $\geq$ 0.4 mm (diameter $\geq$ 0.4 mm) indexes. The discussion section, IV, presents the mean uncertainty of the nidp index, together with the analysis of a sample of patients with anisocoria taken from a paper published in the literature, whereas section V gives the conclusion.

A. CONGENITAL STRABISMUS AND PUPILLOMETRY

Congenital strabismus is the most common form of presentation [19]; it is concomitant and can present inward deviation (esotropia) or outwards (exotropia) [20].

On the other hand, dissociated strabismus is a subtype of congenital strabismus that occurs in both esotropias and exotropias [21], [22]. This paper analyzes patients with dissociated and non-dissociated congenital strabismus. However, many times it is not possible to differentiate dissociated and non-dissociated forms clinically [23]–[25]. Dissociated congenital strabismus manifest slow, variable, and asymmetric movements that can be vertical called Dissociated Vertical Deviation (DVD) or horizontal movements, known as Dissociated Horizontal Deviation (DHD) [26]. Because dissociated movements are manifested by the patients when one eye is occluded or when fixation changes [27], it is believed that the asymmetric input exacerbates them [28], [29]. Dissociated movements have a poor prognosis in the sense of leading to unsatisfactory results [30], [31], compared to non-dissociated forms. The American Academy of Pediatric Ophthalmology concludes that the non-dissociated congenital strabismus has a good aesthetic and functional prognosis, whereas, at the same time, the Cochrane Database Syst Rev study shows discouraging results for the treatment of dissociated congenital strabismus [31]. Several clinical and neuroimaging analyzes show that dissociated congenital strabismus has more significant neurological alterations [32], [33] compared to non-dissociated forms. Neuroimaging studies in the cerebral cortex of strabismic patients corroborate this situation [33], [34]. It is noteworthy to mention that the International Classification of Diseases, Ninth Revision, Clinical Modification (ICD-9-CM) [35], recognize 78 codes typifying different varieties of strabismus [36].

On the other hand, since 1929, the pupillary response has been used for diagnostic and prognostic [37]. Video and infrared light pupilography showed to be a useful tool to detect the effect of some drugs and to analyze Horner syndrome or tonic pupil of Adie [38]. For diagnostic and prognostic purposes, pupilography has several applications, for example, its use in optic neuropathy and afferent pupillary defect [39], in sleep disorders [40], and other diseases [41], [42]. The study performed by Girking [43] evaluated the behavior of both neurological and ophthalmological disorders for diagnostic purposes but, unfortunately, did not address the strabismus issue. Yet, there are no precedents to identify and measure anisocoria in children with congenital strabismus.

II. MATERIALS AND METHODS

This observational, cross-sectional, and prospective study included 168-Mexican children aged 5-15-years from Querétaro, with an established diagnosis of dissociated and non-dissociated congenital strabismus. The ophthalmologist and the staff at the Institute of Congenital Diseases of Querétaro, México, from 2017 to 2018 collected medical records and carried out the clinical examination.

On the other hand, the research presented here conforms to the principles of the Declaration of Helsinki. Any procedure carried out on the patients had the consent of the participants and parents. The number of patients who came to the center

and met the inclusion criteria determined the size of the sample.

Inclusion criteria: diagnosis of dissociated and non-dissociated congenital strabismus; age, 5-15 years.

Exclusion criteria: diagnosis of secondary strabismus (neurological, traumas, diseases), presence of conditions such as Attention-deficit/hyperactivity disorder (ADHD), epilepsy, dyslexia, and depression, use of medication that could affect the central nervous system, and premature birth.

A. IMAGING

The ophthalmologist filmed all patients in scotopic conditions, 0 lux - 0.3 lux, using high sensitivity video with a night vision system based on Night Shot technology incorporated in a Sony digital camera, model DCR-DVD108. A seventy-seven LEDs(wavelength 850 nm) lamp of 5 mm was placed to 2 m in front of the pediatric patients during the experiment. For each recorded video, the camera location was at eye level with the patient in a sitting position facing forward. During the session, children looked at 10 $\times$ 10 cm white target located 2 m away for fixation and accommodation control, to capture both pupils simultaneously. Fig. 1 illustrates the experiment configuration. Then, the ophthalmologist selected and classified several frames. Fig. 2 shows the type of images analyzed in this study.

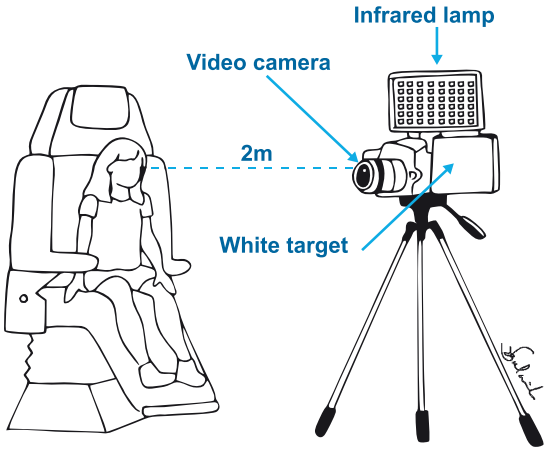

FIGURE 1. Experiment configuration.

The results presented in our paper considered the same illumination condition for each patient. Yet, it is difficult to perform all the examinations in a dark room because there are variations in ambient illumination during the exam since the light emitted from the video-camera display prevented complete darkness [44]. The Fig. 3 in [45], illustrates that the pupil size varies few between 0 lux–0.5 lux, and in Table 1 provided in [44], shows that the prevalence of anisocoria $\geq$ 0.4 mm is the same between 0 lux–0.3 lux. It is noteworthy to mention that the pupil size changes under different conditions, and not only for the illumination but emotional distress, pupillary unrest, among others, provoke changes.

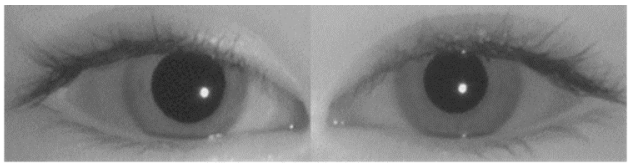

FIGURE 2. The analyzed video frames. These images correspond to the right and left eyes of a patient 10-year-old diagnosed with congenital strabismus. Notice the difference in size and shape of pupils. In this case, the pathological pupil, left eye, presents the smaller size in scotopic conditions.

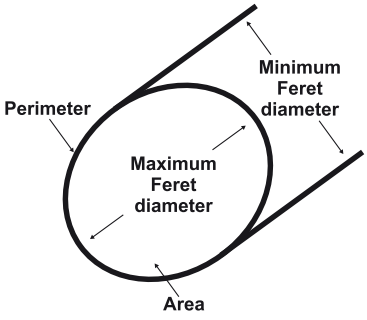

FIGURE 3. Set of parameters utilized in this research [47]. Notice that a circular representation means identical maximum and minimum Feret diameters.

B. SAMPLE TREATMENT

The ophthalmologist analyzed each video sequence and selected the best images to compare both pupils for each patient. The focus, attention, and involuntary movements of the eyes were essential in the selection process to avoid induced miosis due to inadequate placement. It is noteworthy to mention that children were looking straight ahead during the session. The same physician obtained all measures in pixels, and the experiments were at scotopic conditions (0 lux-0.3 lux).

ImageJ software [46] allowed the ophthalmologist to measure maximum and minimum Feret diameters for the corneas and pupils in the selected images. Fig. 3 illustrates these parameters in a general way [46]. The authors used the Excel^{TM} software to compute the proposed indexes manually for the 168 patients, and the Origin^{TM}program allowed researchers to obtain all the graphics.

C. PROPOSALS FOR AN INDIVIDUAL PUPIL ANALYSIS

1) ESTABLISHMENT OF INDICES USING A RATIO OF AREAS

The concept of PP introduced as follows will be useful to identify the difference in size in each analyzed pupil.

Definition 1 (Pattern Pupil PP): Area of a circle whose diameter is equivalent to the average value between the maximum Feret diameter of both pupils.

$$\mathrm{PP} = \frac{\pi[\mathrm{FMPR} + \mathrm{FMPL}]^2}{16} \tag{1}$$

where PP denotes the average area of both pupils, FMPR and FMPL represent the maximum Feret diameter of the right and left pupils, and rpp$= \frac{(\frac{\mathrm{FMPR}}{2} + \frac{\mathrm{FMPL}}{2})}{2} = \frac{\mathrm{FMPR+FMPL}}{4}$ designates the average radius obtained from the Feret diameters of both

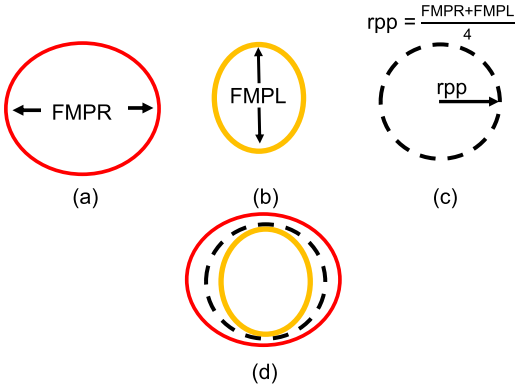

FIGURE 4. Relation of areas among the pupils. (a) and (b) maximum Feret diameter for a hypothetical example considering different sizes for the right and left pupils denoted as FMPR (Feret maximum pupil right) and FMPL (Feret maximum pupil left). The expression $\pi(\text{radius})^2$ allows calculating the areas A_{rp} and A_{lp}; (c) rpp radius obtained from parameters of both pupils, and (d) location of the PP (black) between the edges delimited by both pupils represented in red and orange.

pupils. Fig. 4 provides a hypothetical example showing the parameters appearing in (1). Note that in Fig. 4(d) the PP location is between both pupils.

The iipr and iipl expressions for each pupil in terms of PP are the following.

$$\text{iipr} = \frac{\text{A}_{\text{rp}}}{\text{PP}} \tag{2}$$

$$\text{iipl} = \frac{\text{A}_{\text{lp}}}{\text{PP}} \tag{3}$$

where iipr and iipl represent individual area ratio indexes, for the right and left pupil, respectively, A_{rp} and A_{lp} correspond with the area of the right and the left pupil. If iipr $= 1$ and iipl $= 1$, the pupils have a circular shape with the same size. Otherwise, PP is between both pupils, i.e., there is anisocoria. A comparison using PP with each pupil permits an individual analysis.

The application of (2) and (3) on the set of 168 patients produce several values. Figs. 5(a) and 5(b) show these values sorted in a descending way. Since indexes are area ratios, scale problems are not a problem. Fig. 5(c) illustrates the overlapped iipr and iipl indexes. Whereas Fig. 5(d) shows the arithmetic differences between the iipr and iipl values.

Exist other indexes utilized in several papers, one of them is, for example, the proximity criterion $\rho(x)$, which allows modifying the image contrast [48] through the toggle mappings, and in [49], researchers introduce a pattern to verify the graphite distribution.

2) PUPILS ANALYSIS BASED ON THE DIFFERENCE BETWEEN THE AREA RATIOS

In section II-C1, iipr and iipl indices were introduced, which can provide individual information for each pupil. From (2) and (3), we could deduct the following,

$$\text{nidp} = \text{abs(iipr-iipl)} = \frac{\text{abs}(\text{A}_{\text{rp}} - \text{A}_{\text{lp}})}{\text{PP}} \tag{4}$$

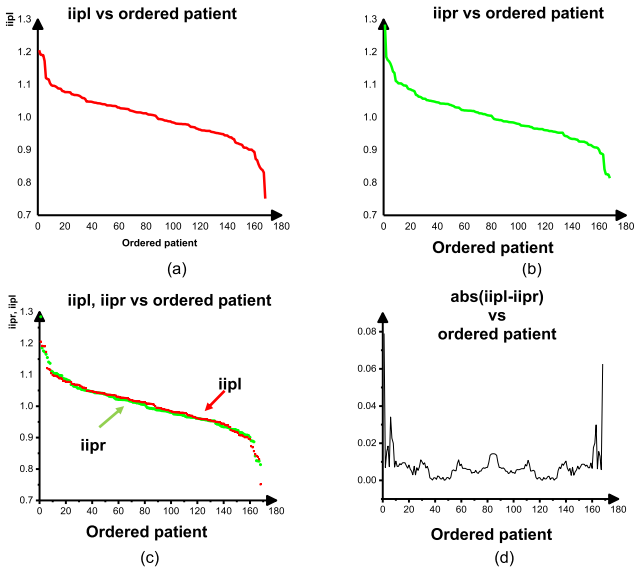

FIGURE 5. iipl and iipr indexes for each pupil. (a) iipl vs. "ordered patient"; (b) iipr vs. "ordered patient"; (c) overlapped graphics (a) and (b); (d) absolute arithmetic difference point by point of the iipl and iipr indexes.

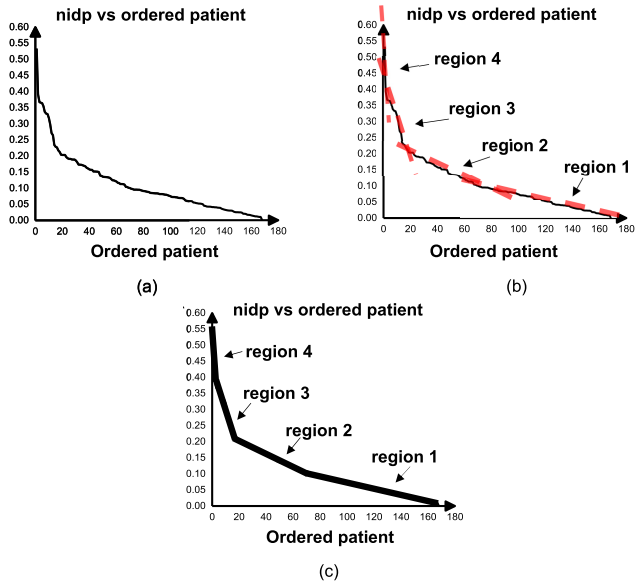

FIGURE 6. Behavior of nidp index. (a) nidp vs. "ordered patient"; (b) four regions detected and delimited with four straight lines on the curve nidp vs. "ordered patient"; (c) mathematical approximation of the function presented in Fig. 6(a) using four straight lines given by (5).

where nidp represents a normalized index based on the area difference between both pupils, and abs() denotes the absolute value. From (4), notice that if the areas of both pupils are equal, nidp $= 0$. However, if nidp $\neq 0$, anisocoria is established because the sizes of pupils are different.

Fig. 6(a) shows the nidp values sorted in descending order. Hence, the nidp index helps to determine distinct degrees of anisocoria. For example, if patient 1 has a nidp_1 value, and patient 2 has nidp_2 with $\text{nidp}_1 > \text{nidp}_2$, then patient 1 presents more anisocoria than patient 2. In Fig. 6(b), the four zones marked in red serve to detect four degrees of anisocoria.

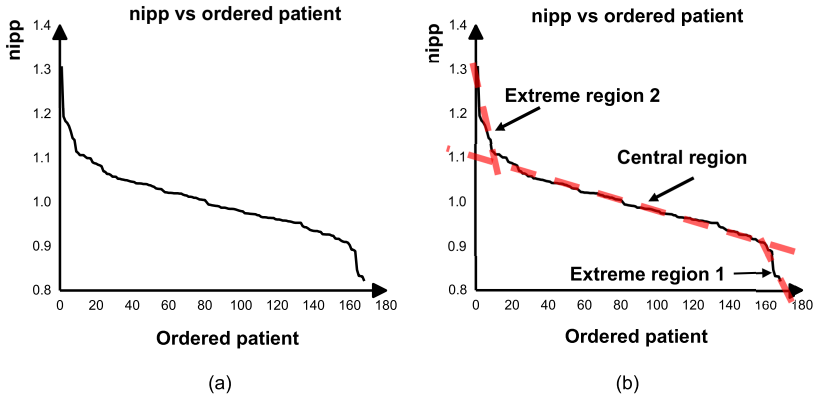

FIGURE 7. The nipp index describes the behavior of pupils in terms of the perimeter. (a) nipp vs. "ordered patient"; (b) three categories of anisocoria detected due to three changes of slope on the curve.

TABLE 1. Coordinates used to build the graph in Fig. 6(c) using the nidp index and the detected degrees of anisocoria. The coordinates belong to the original curve in Fig. 6(a).

Region	("Ordered patient", nidp)	nidp interval	Degree of anisocoria
4	(1,0.533),(3,0.367)	0.367-0.533	VS
3	(3,0.367),(20,0.203)	0.203-0.367	S
2	(20,0.203),(66,0.110)	0.110-0.203	FS
1	(66,0.110),(168,0)	0-0.110	NS

The selection of the straight lines between each intersection comes from the changes in the slope of the graph nidp vs. "ordered patient"; i.e., the red lines changes its direction following the shape of the curve. Also, it is possible to take more or fewer slopes. However, in this paper, we consider that four straight lines give a good approximation to the original curve. Fig. 6(c) presents an estimate of the graph in Fig. 6(a) considering the red lines. Table 1 displays the coordinates used to build the curve in Fig. 6(c). Equation (5) expresses the mathematical function $f(x)$ observed in Fig. 6(c).

$$f(x) = \begin{cases} -0.0831x + 0.5971 & \text{if } 1 \leq x \leq 3 \\ -0.0114x + 0.3935 & \text{if } 3 \leq x \leq 20 \\ -0.0021x + 0.205 & \text{if } 20 \leq x \leq 66 \\ -0.001x + 0.1069 & \text{if } 66 \leq x \leq 168 \end{cases} \tag{5}$$

where x denotes the ordered patient.

The four regions associated with changes in the slope in Fig. 6(c), allows identifying four intervals linked with four degrees of anisocoria. Area 1 contains 102 patients, zone 2 has 46 patients, sector 3 with 17 patients, and 3 patients belong to region 4. The anisocoria detected in Fig. 6 (c) has the next classification: "Very significant" (VS), "Significant" (S), "Few significant" (FS), and "Non-significant" (NS), respectively. Table 1 summarizes the previous information. It is noteworthy to mention that $f(x)$ indicates that anisocoria has a well-defined behavior, and the straight lines have the roll of detecting the threshold values (obtained from the curve in Fig. 6(a)) between each delimited region.

3) INDEX BASED ON THE PERIMETER OF PUPILS

The conventional way to deal with anisocoria is by comparing the perimeters of both pupils. Thus, as a proposal, the next index will be useful to obtain a measure related to the pupil border.

$$\text{nipp} = \frac{\text{prp}}{\text{plp}} \tag{6}$$

nipp represents a normalized index using the perimeters of pupils, prp, and plp denote the length of the rim of the right and left pupils. The graph in Fig. 7 presents the values obtained by applying (6) to the set of patients. The nipp values are in descending order.

From (6), there is anisocoria if nipp $\neq 1$, since if nipp >1 or nipp < 1, the perimeters of both pupils are different. There exists an absence of anisocoria if nipp $= 1$ because both pupils have the same size. Note that, from Fig. 7(a), if nipp $= 1.2$ or nipp $= 0.8171$, this means more anisocoria than if nipp $= 1.01$, because from Fig. 7(b), the values nipp $= 1.2$ and nipp $= 0.8171$, are in the extreme regions of the curve.

Equations (4) and (6) present differences, since the nidp index permits to detect four changes of slope on the curve in Fig. 6(b), that correspond to four degrees of anisocoria, as shown in Fig. 6(c). Whereas in the graph in Fig. 7(a), three changes of the slope on the nipp curve were detected. Regions marked in red represent the three degrees of anisocoria detected using the perimeter of pupils as a criterion. On the other hand, ImageJ [46] software helped to obtain the Feret diameters of both pupils in pixels units. Thus, to express the measures in mm, the following information will be used. The cornea [50] has a horizontal mean diameter of 11.7 mm, and a vertical one of 10.6 mm. In this research, the cornea diameter had a value of 11.7 mm. Nevertheless, the vertical diameter also can be used. Following expression allows to compute the perimeter in mm for each pupil:

$$\text{pmm} = \frac{2(\text{MC})(\text{pxp})}{(\text{drc} + \text{dlc})} \tag{7}$$

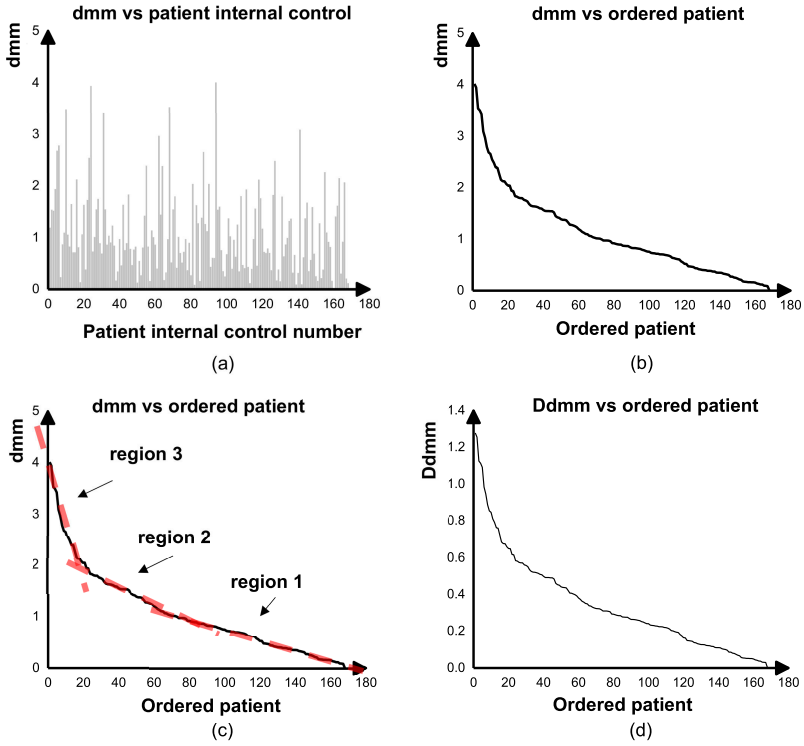

FIGURE 8. The difference in mm of both pupils for the perimeter (dmm) and diameter (Ddmm). (a) The graph dmm vs. "Patient internal control," gives information on the difference in mm of both pupils without an ordering; (b) presents sorted data in a descending way taken from Fig. 8(a); (c) the three detected regions correspond with changes of slope on the curve in Fig. 8(b); (d) difference of diameters Ddmm using (9).

where pxp is the perimeter of the right (prp) or left (plp) pupil in pixels, respectively, drc and dlc denote the horizontal diameters of the right and left corneas obtained with the ImageJ software in pixels. MC represents the mean horizontal diameter of the cornea reported in the literature, i.e., 11.7 mm. Equation (10) allows expressing the difference of both pupils dmm in mm, i.e.;

$$\text{dmm} = \frac{2(\text{MC})}{\text{drc} + \text{dlc}} \text{ abs (prp-plp)} \tag{8}$$

abs() represents the absolute value.

In Fig. 8(a), the parameter dmm is represented graphically for each patient according to their internal control number. The differences go from 0 mm to 4.014 mm within the set of analyzed patients. The sorting in descending order of the perimeters located in Fig. 8(a) yields the graph in Fig. 8(b). In a similar way that in Fig. 7, three regions are distinguished by considering the slope changes of the curve. Fig. 8(c) illustrates this situation. Table 2 provides the coordinates to detect the three degrees of anisocoria following the regions delimited by the three straight lines displayed in Fig. 8(c).

The three regions associated with changes in the slope in Fig. 8(c) correspond with three intervals linked with three degrees of anisocoria, VS, S, and NS, respectively. Region 1 contains 78 patients; zone 2 has 71 patients; and sector 3 with 19 patients. Table 2 presents such information.

TABLE 2. Intervals and degrees of anisocoria using the difference of perimeters dmm obtained from Fig. 8(c).

Region	("Ordered patient", dmm)	dmm interval	Degree of anisocoria
3	(1,4.013),(19, 2.071)	2.071-4.013	VS
2	(19,2.071),(90,0.828)	0.828-2.071	S
1	(90,0.828),(168,0)	0-0.828	NS

From (8), to calculate the difference between the diameters of the right and left pupil in mm, denoted as Ddmm, the π value should divide the expression, i.e.,

$$\text{Ddmm} = \frac{2(\text{MC})}{\pi(\text{drc} + \text{dlc})} \text{ abs(prp-plp)} \tag{9}$$

Fig. 8(d) shows the graphic representation by ordering in a descending way the Ddmm values for the analyzed patients. Following the same analysis given in this paper, Table 3 shows the information obtained from the changes on the slope of the curve in Fig. 8(d), which is similar to the plot in Fig 8(c) but divided by π. It is noteworthy to mention that, Fig. 8(d) and Table 3 provide information about the diameter $\geqslant$ 0.4mm to detect anisocoria. Considering the criterion of 0.4 mm of difference between both pupils, 57 patient fulfills such standard, and there are 111 without anisocoria. Nevertheless, the changes in slope on the curve in Fig. 8(d) (equal to the perimeter) indicate that 19 patients are in region 1 classified with a VS degree of anisocoria, 71 with S in zone 2, and 78 with NS in area 3.

TABLE 3. Intervals and degrees of anisocoria using the difference of diameters Ddmm obtained from Fig. 8(d).

Region	("Ordered patient", Ddmm)	Ddmm interval	Degree of anisocoria
3	(1,1.277),(19, 0.659)	0.659-1.277	VS
2	(19,0.659),(90,0.263)	0.263-0.659	S
1	(90,0.263),(168,0)	0-0.263	NS

TABLE 4. 55 random nidp indexes corresponding to the group G of patients with A = dissociated congenital strabismus, and B = non-dissociated congenital strabismus, PN represents the patient number, and AD denotes de anisocoria degree.

PN	G	nidp	AD	PN	G	nidp	AD
3	A	0.18579	FS	61	B	0.00902	NS
7	A	0.02484	NS	65	B	0.19244	FS
8	A	0.06887	NS	67	B	0.02458	NS
10	A	0.36551	S	68	B	0.03176	NS
20	A	0.09527	NS	70	B	0.39185	VS
24	A	0.3315	S	72	B	0.16786	FS
63	A	0.05158	NS	74	B	0.04491	NS
69	A	0.11225	FS	77	B	0.05487	NS
78	A	0.07503	NS	80	B	0.04232	NS
114	A	0.17261	FS	81	B	0.07954	NS
130	A	0.15685	FS	86	B	0.16947	FS
119	A	0.15822	FS	88	B	0.13221	FS
140	A	0.13454	FS	90	B	0.11584	FS
1	B	0.13475	FS	95	B	0.05939	NS
2	B	0.1611	FS	99	B	0.00232	NS
4	B	0.18926	FS	104	B	0.17322	FS
9	B	0.10405	NS	105	B	0.10369	NS
11	B	0.09383	NS	117	B	0.04003	NS
12	B	0.07222	NS	124	B	0.08969	NS
19	B	0.012	NS	135	B	0.19089	NS
36	B	0.08392	FS	136	B	0.05461	NS
39	B	0.01937	NS	141	B	0.03087	NS
44	B	0.09224	NS	147	B	0.05916	NS
47	B	0.07116	NS	148	B	0.12894	FS
48	B	0.03905	NS	149	B	0.15695	FS
53	B	0.0234	NS	153	B	0.08478	NS
54	B	0.08147	NS	154	B	0.02439	NS
58	B	0.01378	NS				

TABLE 5. Analysis of ANOVA to detect two types of congenital strabismus, dissociated and non-dissociated.

Source	DF	Adj SS	Adj MS	F-Value	p-Value
Group	1	0.03235	0.032346	4.96	0.03
Error	53	0.34596	0.006527		
Total	54	0.3783			

The nidp index detected 4 degrees of anisocoria by analyzing 168 patients with two types of congenital strabismus. ANOVA analysis allows identifying a significant difference between patients with dissociated and non-dissociated congenital strabismus. As mentioned previously, the dissociated strabismus has more significant neuronal implications than the non-dissociated variety [33], [51]–[54]. For this, the Minitab program analyzed a random sample of 55 files taken from the 168 studied patients. Table 4 displays the data set. The null hypothesis is "All means are equal," and the alternative one, "Not all means are equal," with a significance level $\alpha = 0.05$. Table 5 shows the analysis of variance, and Table 6 the Fisher pairwise comparison.

From the analysis of ANOVA, is discarded the null hypothesis since $p = 0.03$. Thus, A and B groups are different,

TABLE 6. Grouping information using the Fisher LSD method and 95% confidence. The analysis detects the two types of congenital strabismus, dissociated (A) and non-dissociated (B).

Group	N	Mean	Grouping	
A	13	0.1487	A	
B	42	0.0916		B

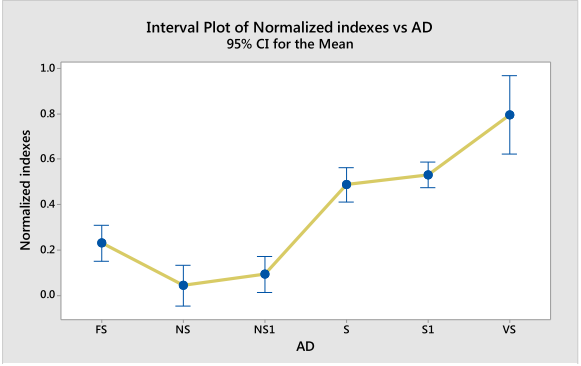

FIGURE 9. Comparison among the groups of anisocoria NS, FS, S, VS, NS1 and S1, detected using the nidp and Ddmm ≥ 0.4 mm indexes and classified according to the the Tukey method.

and the pairwise comparison of Fisher provides the mean values for each group. The group A has a mean value more significant than group B. Thus, nidp values permit found through ANOVA the existence of the two groups of congenital strabismus analyzed in this paper. The second ANOVA study analyzed 88 samples to compare the anisocoria degree recognized by the nidp and Ddmm $\geq$ 0.4mm indexes. Due to indexes have different ranges, they were normalized using the following equation:

$$\text{normalized value} = 1 - \text{abs}\left(\frac{\text{index-Max}}{\text{Min-Max}}\right) \tag{10}$$

Max and Min denote the maxima and minima values for the analyzed sample corresponding to nidp and Ddmm indexes, and abs() indicates the absolute value. Table 7 displays the data set. Nndip and NDdmm represent the normalized indexes, and they take their values between 0-1. From Table 8, the p-value indicates that there are differences in the analyzed degrees of anisocoria, and Table 9 shows the comparison among the groups.

Note from Fig. 9 that both indexes nidp and Ddmm detect "No Significant" and "Significant" anisocoria in a similar way, but nidp is superior to Ddmm $\geq$ 0.4 mm because it also recognizes the "Few significant" and "Very significant" degrees of anisocoria.

III. RESULTS

The definition of PP permits the introduction of the iipr and iipl indexes expressed in (2) and (3), respectively. This step was necessary because there is not a standard size of human pupils. These indices allowed setting normalized values which have the advantage of being invariant to the scale of the image. The study revealed that pupils present problems of size and deformity when compared with the pattern built with

TABLE 7. 88 samples to compare the anisocoria degrees (AD) between NDdmm and Nnidp values. Where NDdmm = normalized Ddmm ≥ 0.4 mm, and Nnidp = normalized nidp index. PN represents the patient number. The anisocoria degrees detected by the nidp index are, NS = "No significant", FS = "Few significant", S = "Significant", VS = "Very Significant". The anisocoria degrees detected by the Ddmm ≥ 4 mm index are, S1 = "Significant", and NS1 = "No significant".

PN	AD nidp	nidp	Nnidp	AD for Ddmm ≥ 0.4 mm	Ddmm	NDdmm
1	FS	0.1348	0.2053	NS1	0.38	0.2347
5	S	0.2641	0.4632	S1	0.8539	0.6387
6	S	0.337	0.6083	S1	0.8869	0.6669
10	S	0.3655	0.6652	S1	1.1129	0.8595
13	FS	0.1964	0.328	S1	0.5255	0.3587
15	NS	0.0693	0.0748	NS1	0.2281	0.1052
17	S	0.2174	0.3701	S1	0.6767	0.4876
20	NS	0.0953	0.1266	NS1	0.3383	0.1991
21	FS	0.1393	0.2143	S1	0.5206	0.3545
25	S	0.3641	0.6625	S1	1.2554	0.981
29	FS	0.1888	0.3129	S1	0.5574	0.386
32	S	0.3545	0.6432	S1	1.0907	0.8406
41	FS	0.1128	0.1616	NS1	0.3099	0.1749
42	NS	0.0418	0.02	NS1	0.1475	0.0365
48	NS	0.039	0.0145	NS1	0.1492	0.0379
55	FS	0.1245	0.1849	S1	0.4533	0.2972
56	S	0.2714	0.4776	S1	0.762	0.5603
64	S	0.3179	0.5703	S1	0.9465	0.7176
65	FS	0.1924	0.3203	S1	0.4602	0.3031
66	S	0.2286	0.3924	S1	0.7595	0.5583
68	NS	0.0318	0	NS1	0.1047	0
69	FS	0.1123	0.1604	NS1	0.3085	0.1737
70	VS	0.3918	0.7177	S1	1.125	0.8698
83	S	0.2341	0.4034	S1	0.649	0.464
88	FS	0.1322	0.2002	S1	0.4413	0.2869
89	VS	0.5335	1	S1	0.8459	0.6319
92	S	0.2031	0.3415	S1	0.6493	0.4643
93	NS	0.0406	0.0177	NS1	0.1388	0.0291
96	VS	0.3672	0.6686	S	1.2777	1
104	FS	0.1732	0.2819	S1	0.4378	0.2839
105	NS	0.1037	0.1434	NS1	0.3266	0.1892
111	S	0.2121	0.3595	S1	0.5748	0.4007
120	NS	0.0384	0.0132	NS1	0.146	0.0352
121	S	0.2031	0.3415	S1	0.6759	0.487
122	FS	0.1511	0.2379	S1	0.5609	0.3889
129	NS	0.0387	0.0138	NS1	0.1176	0.011
131	S	0.2981	0.5308	S1	0.7912	0.5852
139	FS	0.1356	0.2069	S1	0.4212	0.2698
145	S	0.3302	0.5948	S1	0.9843	0.7499
151	NS	0.0508	0.038	NS1	0.1811	0.0651
156	FS	0.1336	0.2029	S1	0.4065	0.2573
158	NS	0.0402	0.0168	NS1	0.1212	0.014
165	FS	0.1378	0.2113	S1	0.4496	0.2941
167	S	0.2265	0.3882	S1	0.6854	0.495

TABLE 8. Analysis of ANOVA using 88 samples to compare the anisocoria degrees (AD) between NDdmm and Nnidp values.

Source	DF	Adj SS	Adj MS	F-Value	P-Value
AD	5	4.041	0.80824	35.45	0.000
Error	82	1.869	0.02280		
Total	87	5.911			

the maximum Feret diameter. The parameters A_{rp} and A_{lp} allow detecting the differences for each pupil individually. Fig. 5 illustrates this situation. The A_{rp} and A_{lp} values corresponding to the right and left pupils are almost overlapped, with minimal differences, as is shown in Fig. 5c. It follows that an analysis based on the differences between the area ratios yielded the nidp index as a result. From the graph nidp vs. "ordered patient," the changes of the slope in the curve allowed distinguishing different degrees of anisocoria into four groups or regions, as depicted in Fig. 10(c). Tables 1, 2, and 3 provide the points to get the threshold defining each interval of anisocoria for the area, perimeter, and diameter.

TABLE 9. Grouping information using the Tukey method and 95% confidence among NS, FS, S, VS, NS1, and S1 anisocoria degrees.

AD	N	Mean	Grouping			
VS	3	0.795	A			
S1	30	0.5313	A	B		
S	16	0.4883		B		
FS	14	0.2306			C	
NS1	14	0.0933			C	D
NS	11	0.0435				D

The following information corresponds to the nidp index (see Fig. 6). Region 1 contains 102 patients (66 to 168 in x-axis), and the magnitude of anisocoria is NS. The alteration in 46 individuals from the second interval (20 to 66 in x-axis) was FS. The third detected interval contains 17 patients (3 to 20 in x-axis) with S magnitude of anisocoria. The fourth interval had 3 patients (1 to 3 in x-axis), and the alteration was VS. Fig. 10(c) summarizes this information. Except for one case, the entire sample showed differences in the size and shape of pupils. However, these differences are not always significant enough to be classified as "anisocoria." From Fig. 10(c), 11.9% of the sample group (20 patients within the regions S and VS) showed a considerable degree of anisocoria whereas the 88.1% (148 patients within the intervals NS and FS) have differences in size and shape of pupils not usually detected using the perimeter or diameter as a standard. In Fig. 10(a), notice that 11.3% of the patients had VS alterations, 42.26% of the sample had S changes, and 46.44% of the patients presented NS alterations. On the other hand, the same percentages of the perimeter curve correspond to the diameter. The diameter ≥ 0.4 mm indicates that 33.9% of the group had anisocoria, see Fig.10(b). By comparing the information provided in Figs. 10(a) – 10(c), a better distribution of the degrees of anisocoria corresponds to the graph in Fig. 10(c). According to the ANOVA experiment, index nidp helps to find the two types of congenital strabismus used in this study. Fig 9 illustrates that the nidp index has a better performance than Ddmm ≥ 0.4 mm criterion because nidp parameter can detect subtle changes of anisocoria.

IV. DISCUSSION

Patients with Syndrome of Horner and third nerve palsy have the characteristic of present notable differences in the size of the pupils, and physicians identify anisocoria without a pupillometer since it is observable under any light condition [55]. These types of anisocorias usually exceed the 0.4 mm, and researchers have described them in the current literature for many years [56]. Whereas for the congenital strabismus, anisocoria is subtle, and many times go unnoticed, which does not occur with the syndrome of Horner. Furthermore, in congenital strabismus, anisocoria is better detected by the specialist in scotopic conditions [9].

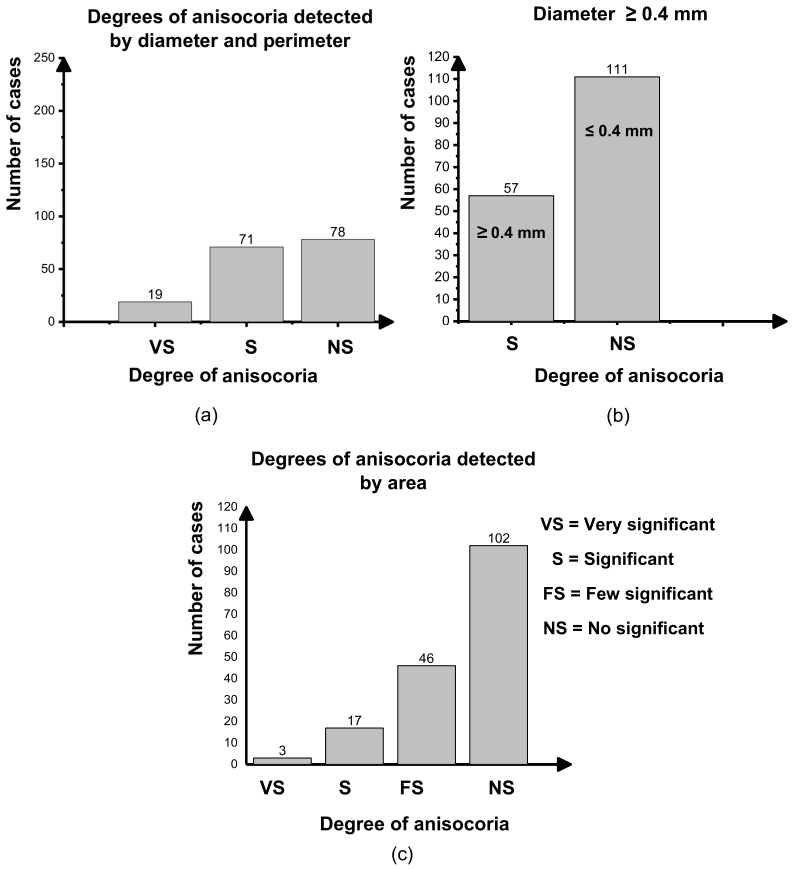

FIGURE 10. Degrees of anisocoria detected utilizing diameter, perimeter, area of pupils and the diameter ≥ 0.4 mm. (a) anisocoria detected using indexes dmm and Ddmm (perimeter and diameter), (b) anisocoria detected using diameter ≥ 0.4mm, (c) anisocoria detected using index nidp (area).

The importance of this study is to provide a more accurate method to determine morphometric parameters of pupils to applying in congenital strabismus, refractive, and cataract surgery. Several ways reported in the literature serve to measure different characteristics of the iris or the pupils. For example, optical coherence estimates the thickness of the tissue in diseases such as glaucoma [57]. For measuring the diameter of pupils, the specialists usually use pupillometers [6].

On the other side, some aspects must be overcome or standardized to study anisocoria. For example, it would be useful to set standards regarding the illumination, the relative dimensions of pupils, rotation and size of the eyes, the distance and angle of the observer, the shape pupils, the anterior chamber depth, patient age, mood, attention, visual acuity, among others [7], [58]. In this sense, analytical methods are better than empirical ones. A clear example is a picture of pupils captured and processed with a smartphone using an app. This procedure is more efficient and decreases human error compared with the experience [6]. The size and shape of the human pupils vary for each individual, hence the need for a more precise method to calculate them, i.e., the image processing technique [59].

In this paper, the pattern pupil concept in terms of the Feret diameter allows for better estimations of the size of pupils. The proposed model allows getting small differences in the pupils of patients diagnosed with congenital strabismus.

Congenital strabismus has some useful characteristics, i.e., as a biological model, it easily separates the visual function from the left and right, facilitating the measurement of each sensory and motor aspects with absolute precision.

The first ANOVA test showed that based on the measurement of anisocoria using nidp, it is feasible to distinguish between the dissociated and non-dissociated congenital strabismus with a significant statistical possibility. This clear distinction can be an aid in the decision-making of the physician when establishing a diagnosis, therapy, or prognosis. Whereas the second ANOVA analysis compared the different degrees of anisocoria detected by the nidp and Ddmm $\geq$ 0.4 mm indexes. Both methods detect in a similar way ''No significant'' and ''Significant'' anisocoria. However, the nidp parameter recognizes the other two intervals, the ''Few significant'' and ''Very significant''. Thus nidp index detects subtle changes not identified by the Ddmm parameter. It is worth mentioning that the changes in the cortical integrator and the pupil size in congenital strabismus are subtle and,

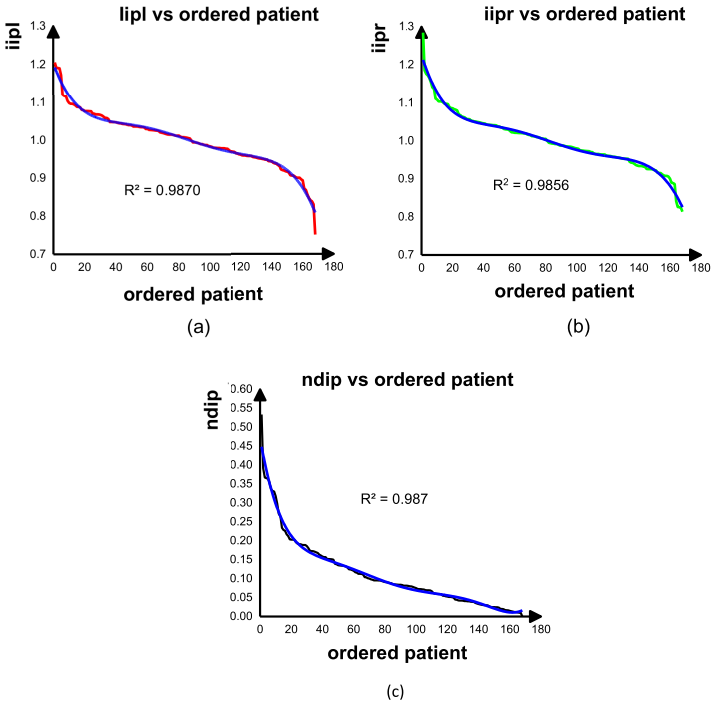

FIGURE 11. Polynomial regression degree 6. (a),(b),(c) Polynomial (blue) computed from the curves iipl (red), iipr (green) and nidp (black) and R^2 parameter.

therefore, difficult to assess. The pupil size varies if the congenital strabismus is dissociated or non-dissociated. And it also varies due to different conditions, for example, mood, some other illness, nervousness, lack of rest, perhaps due to the degree of strabismus as well, which has not been verified by any method described in the literature. This set of variables explain in part, the appearance of FS and NS within the dissociated and non-dissociated congenital strabismus. On the other hand, there are subtypes such as esotropias or exotropias, and it is feasible that these combinations influence the presentation of the different pupil sizes found in our study. For this reason, further study is necessary for the nidp index, which provides four ways of detecting anisocoria, unlike the traditional mode ≥ 0.4 mm.

Another critical point to consider is the border of pupils. The irregularities in the edge of the pupil produce erroneous measures of the perimeter [60] when it is captured directly on the image. In our case, the Feret diameter allows computing it. The area yields better results since more pixels intervene during the calculation. This study shows that the nipp index is less sensitive when compared to the nidp index.

Two strategies we followed had better results. The first action consisted of replacing the diameter with the area of pupils. The second took into consideration the proportion of the areas, where the PP parameter plays a key role. The independent analysis of each pupil allowed calculating the difference between both areas as a parameter. Fig 6(b) shows this situation.

Note the discrepancy in the size of both pupils, either using the area, perimeter, or diameter. In the analyzed sample, pupils do not reach the value of the pattern pupil. The same behavior occurs for the iipr and iipl indexes presented in Fig. 5. In Fig. 5(c), the left pupils show more asymmetry than the right ones.

The curve slope changes in Fig. 6(c) indicates that the more complex cases belong to the patients located in regions 3 and 4. Hence, higher values of nidp than 0.203, correspond with a higher anisocoria. The subtlest differences occurred in groups of patients located in regions 1 and 2. However, this does not mean that these patients have no medical problems. Tables 1, 2, and 3 summarize the information of the nidp (area differences), dmm (perimeter differences), and Ddmm (diameter differences) indexes obtained from Figs. 6(c) and 8(c), respectively. When comparing the column ''degree of anisocoria'' in Tables 1, 2, and 3, the indexes associated with the perimeter and diameter do not allow to distinguish subtle changes in pupil size. A more critical situation occurs for the diameter > 0.4mm to measure anisocoria because the threshold detects two regions. Fig. 10(b) illustrates this situation. Hence, the perimeter, diameter, and the diameter ≥ 0.4 mm do not give good results when contrasted with those obtained from the area. However, the indexes dmm (perimeter) and Ddmm (diameter), give better results than the diameter ≥ 0.4mm to detect anisocoria.

Note that the Feret diameter for each pupil measured by the ophthalmologist is ground truth. The polynomial regression

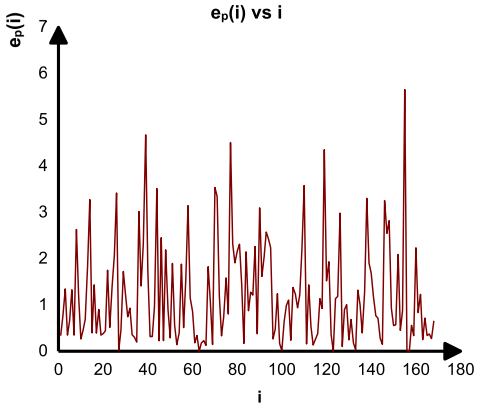

FIGURE 12. $e_p(i)$ with i = 1,...,168, mean 1.2083, SE mean 0.0834, StDev 1.0807. These values were computed using MiniTab™ software.

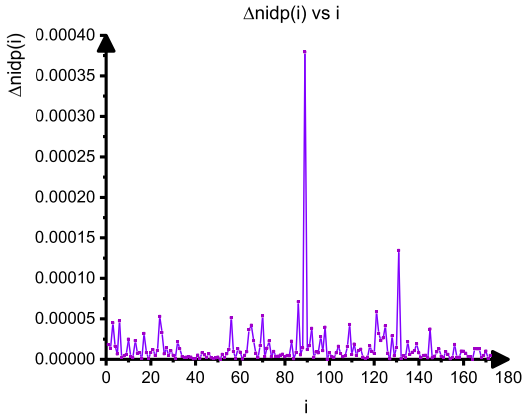

FIGURE 13. Uncertainties computed for the nipd(i) indexes, with i = 1...168, using StDev 1.0807.

of iipr, iipl, and nidp indexes is computed and presented in Fig. 11. The high value of R^2 indicates that: 1) the ophthalmologist recollected the data carefully, 2) the error is small because the indices involve the arithmetic subtraction and are normalized.

However, there is an associated error during the measurement. Thus the percentage error formula (11) will help to obtain it [61] together with (12),

$$e_p(i) = \frac{V_r - V_m(i)}{V_r} \times 100 \tag{11}$$

where V_r denotes the real value, $V_m(i)$ the measures done, and $i = 1,..,n = 168$ (number of patients). Let be $V_m(i) = drc(i)$ and $V_r = MC$ (fixed mean value [50]),

$$MC = \frac{drc(i) + dlc(i)}{2} \tag{12}$$

Fig. 12 shows the $e_p(i)$ computed for the 168 nidp indexes.

Fig. 13 displays the uncertainties for the nidp indexes with 0.000014 as the mean uncertainty. The calculated uncertainties utilized the formulas of multiplication and division for systematical errors [62]. For example, consider the nidp(1) value with its respective uncertainty,

TABLE 10. Data obtained from [63].

Age group	Average pupil size (mm)	Average anisocoria (mm)
0-3	5.309	0.25
4-7	5.8688	0.23
8-11	6.07522	0.24
12-15	6.1242	0.31
16-17	6.2402	0.44

TABLE 11. Estimation of diameter left pupil, PP, iipr, iipl, and nidp. Where, Diameter left pupil = Diameter right pupil-Average pupil size.

Right pupil diameter (mm)	Left pupil diameter (mm)	PP	iipr	iipl	nidp
5.309	5.059	21.106	1.048	0.952	0.096
5.868	5.638	26.001	1.040	0.960	0.079
6.075	5.83522	27.853	1.040	0.960	0.080
6.124	5.814	27.984	1.052	0.948	0.103
6.240	5.800	28.465	1.074	0.928	0.146

i.e., nidp(1) = 0.12899 ± 1.80e-05, thus 0.128972 ≤ nidp(1) ≤ 0.129008, and the variation is less than 0.01 %. On the other side, nidp is approximated by (5). The graph in Fig. 6(c) illustrates the following: i) the four regions delimiting the 4 degrees of anisocoria, and ii) provide the threshold values for each detected region in axis x.

Equation (13) allows computing the e_{rms} value between the nidp and the values originated by the four straight lines in (5), this is 0.06, and data have a StDev = 0.0017

$$e_{rms} = \sqrt{\frac{1}{168}\sum_{x=1}^{168}(\text{nidp}(x) - f(x))^2} \tag{13}$$

In this case, the uncertainty $\Delta(X \pm Y) = \sqrt{\Delta X^2 + \Delta Y^2} =$ 0.0024 is higher because the difference is not normalized.

On the other hand, in [63], the authors illustrated the performance of the digital pupillometer plusoptiX GmbH measuring the pupil size on a sample group of 1306 children aged 0-17 years to verify two things, 1) that the pupil size increase with age and 2) the incidence of anisocoria ≥ 0.4 mm. The research showed that 19.1% of the sample group had anisocoria ≥ 0.4 mm. Table 10 displays the average quantities used in that paper. The quantities of the column "Average pupil size," was obtained from a bar chart presented in [63] using the software WebPlotDigitizer-4.2-win32-x64. These values allowed computing the nidp index using (4). It is worth mentioning that the analysis of the mean values gives a good idea about anisocoria. Table 11 displays the PP, iipr, iipl, and nidp values calculated from (1), (2), (3) using the information presented in Table 10.

Fig. 14 shows the nidp values ordered in a descending way, and Table 12 gives the anisocoria degree using the information of Table 1. The mean data reported in [63], have the next interpretation according to our proposal. The analysis lets to distinguish two types of anisocoria, VS, and S, but not subtle changes. This situation may occur because the authors in [63] introduced the plusoptiX GmbH, and utilized pupils of considerable dimension to detect the diameters with precision. According to the nidp index, 100% of the sample group has anisocoria with degrees VS and S. This result has

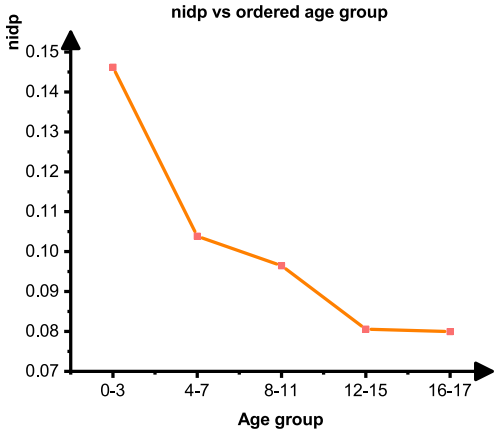

FIGURE 14. nidp values computed for each age group.

TABLE 12. Anisocoria degree detection using Table 1.

Ordered age group	nidp	Anisocoria degree
16-17	0.146	VS
12-15	0.103	VS
0-3	0.096	S
8-11	0.080	S
4-7	0.079	S

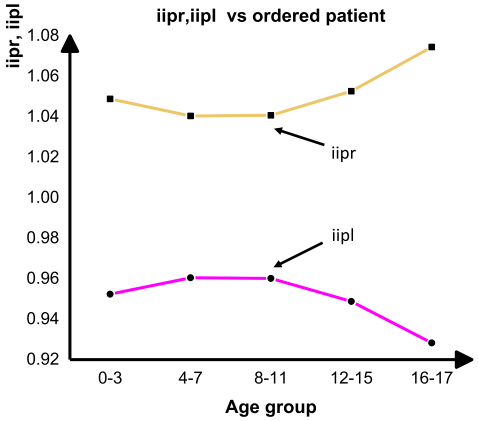

FIGURE 15. Age group Anisocoria trend.

sense because the authors measure anisocoria ≥ 0.4 mm. In [63], the authors showed that pupil size increases with age. However, anisocoria does not have linear behavior; indexes iipr and iipl indicate a parabolic trend. Fig. 15 illustrates this situation.

V. CONCLUSION

The proposed indices involving the mean area of pupils allow better measurement because more pixels and information participate in the calculation, and detect more anisocoria degrees than those identified when using the perimeter, or diameter.

On the other hand, the PP concept allows analyzing each pupil independently. Moreover, the proposed indices can be implemented readily by the reader. The study showed that except in one case, there are no circular pupils. Concerning the circular pattern used as a reference, Figure 4(c), both eyes had alterations in shape and size. The above is not possible to detect by using the perimeter or diameter.

Congenital strabismus is an ideal biological model to test the proposal given in this paper because the cortical disorders of congenital strabismus are subtle and difficult to demonstrate using traditional neuroimaging methods. Neurological manifestations are an exacerbation of some oculomotor reflexes, and pupillary changes are subtle. Our study suggests that, at least in congenital strabismus, pupillary asymmetry in shape and size could help to pinpoint the diagnosis and establish the prognosis of the disease. This situation occurs because the ANOVA test showed the existence of two groups of congenital strabismus detected with the help of the nidp index with a significant p-value.

On the other side, our methodology analyzed the findings published in [63]. The nidp index detected three things, 1) the high pupil size used in that experiment to get precision measures with the pupillometer utilized, 2) two anisocoria degrees VS, and S; and 3) the anisocoria presents a parabolic trend with age. These findings show the high performance of the proposal given in this paper. In the future, we will take the following steps, i) our research team will implement an automated process using supervised machine learning instead of a threshold value to classify the patients according to the anisocoria degree they present; ii) further study in the nidp index to detect more types of congenital strabismus.

ACKNOWLEDGMENT

The authors are thankful for UAQ, CONACyT, and PRODEP for the support with the laboratory, scholarship, and financial resources of this research. Also, we acknowledge the edition of figures by Hugo Rodríguez.

REFERENCES

[1] S. A. Kennedy, J. Noble, and A. M. F. Wong, "Examining the pupils," *Can. Med. Assoc. J.*, vol. 185, no. 9, p. E424, Jun. 2013.
[2] L. Chen, J. C. Yeung, and D. R. Anderson, "Anisocoria secondary to anticholinergic mydriasis from homeopathic pink eye relief drops," *Clin. Med. Res.*, vol. 15, nos. 3–4, pp. 93–95, Dec. 2017.
[3] J. Q. Truong and K. J. Ciuffreda, "Quantifying pupillary asymmetry through objective binocular pupillometry in the normal and mild traumatic brain injury (mTBI) populations," *Brain Injury*, vol. 30, no. 11, pp. 1372–1377, Sep. 2016.
[4] J. R. Gross, C. M. McClelland, and M. S. Lee, "An approach to anisocoria," *Current Opinion Ophthalmol.*, vol. 27, no. 6, pp. 486–492, Nov. 2016.
[5] H. Wilhelm, T. Peters, H. Lädtke, and B. Wilhelm, "The prevalence of relative afferent pupillary defects in normal subjects," *J. Neuro-Ophthalmol.*, vol. 27, no. 4, pp. 263–267, Dec. 2007.
[6] D. K. Mojumder, S. Patel, K. Nugent, J. Detoledo, J. Kim, N. Dar, and H. Wilms, "Pupil to limbus ratio: Introducing a simple objective measure using two-box method for measuring early nisocoria and progress of pupillary change in the ICU," *J. Neurosciences Rural Pract.*, vol. 6, no. 02, pp. 208–215, Feb. 2015.
[7] S. Gholami, N. J. Reus, and T. J. T. P. van den Berg, "The significance of changes in pupil size during straylight measurement and with varying environmental illuminance," *J. Optometry*, vol. 11, no. 3, pp. 167–173, Jul. 2018.
[8] R. F. Multack, W. C. Lannin, and J. R. Olbum, "Improving diagnostic acumen in pupillary evaluation: A review for the primary care physician," *J. Amer. Osteopathic Assoc.*, vol. 89, no. 7, pp. 917–924, 1989.
[9] M. Gallegos-Duarte, "Dissociated vertical divergence," *Strabismus*, vol. 20, no. 1, pp. 31–32, Mar. 2012.
[10] J. Lemos and E. Eggenberger, "Neuro-ophthalmological emergencies," *Neurohospitalist*, vol. 5, no. 4, pp. 223–233, Oct. 2015.

[11] T. A. Shazly and G. R. Bonhomme, "A simple infrared-augmented digital photography technique for detection of pupillary abnormalities," *Graefe's Arch. Clin. Experim. Ophthalmol.*, vol. 253, no. 3, pp. 487–490, Mar. 2015.

[12] T. Krzizok, M. Gräf, and S. Kraus, "Photo-and videographic determination of the dilatation deficit in differential diagnosis of horner syndrome," *Der Ophthalmologe: Zeitschrift der Deutschen Ophthalmologischen Gesellschaft*, vol. 92, no. 2, pp. 125–131, 1995.

[13] C. L. Kramer, A. A. Rabinstein, E. F. M. Wijdicks, and S. E. Hocker, "Neurologist versus machine: Is the pupillometer better than the naked eye in detecting pupillary reactivity," *Neurocritical Care*, vol. 21, no. 2, pp. 309–311, Oct. 2014.

[14] C. Dunlop, "Ipsilateral pupil dilation associated with unilateral intermittent exotropia: A new observation," *Clin. Experim. Ophthalmol.*, vol. 39, no. 8, pp. 839–841, Nov. 2011.

[15] T. Wermund, C. Schmidt, and H. Wilhelm, "Characteristics of pupil function in patients with dissociated vertical divergence," *Klinische Monatsblatter Augenheilkunde*, vol. 229, no. 11, pp. 1090–1096, 2012.

[16] J. V. Haxby, "Multivariate pattern analysis of fMRI: The early beginnings," *NeuroImage*, vol. 62, no. 2, pp. 852–855, Aug. 2012.

[17] P. Zeidman, A. Jafarian, N. Corbin, M. L. Seghier, A. Razi, C. J. Price, and K. J. Friston, "A guide to group effective connectivity analysis, part 1: First level analysis with DCM for fMRI," *NeuroImage*, vol. 200, pp. 174–190, Oct. 2019.

[18] J. M. Marti-Climent, E. Prieto, J. L. López, and J. Arbizu, "Neuroimaging: Technical aspects and practice," *Revista Española Med. Nuclear*, vol. 29, no. 4, pp. 189–210, 2010.

[19] P. Sharma, N. Gaur, S. Phuljhele, and R. Saxena, "What's new for us in strabismus?" *Indian J. Ophthalmol.*, vol. 65, no. 3, p. 184, 2017.

[20] D. T. Oystreck and C. J. Lyons, "Comitant strabismus: Perspectives, present and future," *Saudi J. Ophthalmol.*, vol. 26, no. 3, pp. 265–270, Jul. 2012.

[21] E. C. Engle, "Genetic basis of congenital strabismus," *Arch. Ophthalmol.*, vol. 125, no. 2, pp. 189–195, 2007.

[22] Y. Pang, K. A. Frantz, and D. G. Schlange, "Vision therapy management for dissociated horizontal deviation," *Optometry Vis. Sci.*, vol. 15, p. 1, Oct. 2012.

[23] P. Loba and A. Broniarczyk-Loba, "Difficulties in diagnosis and treatment of dissociated vertical deviation DVD. Part I," *Klinika Oczna*, vol. 109, nos. 7–9, pp. 356–358, 2007.

[24] UFO Themes. (2016). *Dissociated Strabismus Complex*. Accessed: May 24, 2020. [Online]. Available: https://entokey.com/dissociated-strabismus-complex

[25] I. D. Apăatăachioae, A. Băarar, G. Vintilăa, and C. Apăatăachioae, "Dissociated horizontal deviation—A diagnostic problem in strabismus," *Oftalmologia*, vol. 50, no. 1, pp. 63–69, 2006.

[26] A. Christoff, E. L. Raab, D. Guyton, M. C. Brodsky, K. J. Fray, K. Merrill, C. C. Hennessey, E. D. Bothun, and D. G. Morrison, "DVD a conceptual, clinical, and surgical overview," *J. Amer. Assoc. Pediatric Ophthalmol. Strabismus*, vol. 18, no. 4, pp. 378–384, 2014.

[27] R. Ghadban, L. Liebermann, L. D. Klaehn, J. M. Holmes, and M. C. Brodsky, "Relative roles of luminance and fixation in inducing dissociated vertical divergence," *Investigative Ophthalmol. Vis. Sci.*, vol. 56, no. 2, pp. 1081–1087, Feb. 2015.

[28] M. P. M. ten Tusscher and R. J. van Rijn, "A hypothetical mechanism for DVD: Unbalanced cortical input to subcortical pathways," *Strabismus*, vol. 18, no. 3, pp. 98–103, Sep. 2010.

[29] L. J. van Rijn, M. P. M. ten Tusscher, I. de Jong, and F. Hendrikse, "Asymmetrical vertical phorias indicating dissociated vertical deviation in subjects with normal binocular vision," *Vis. Res.*, vol. 38, no. 19, pp. 2973–2978, Oct. 1998.

[30] C. M. Sánchez-Valdés, C. E. Murillo-Correa, and A. C. Baca-Ruíz, "Aparición de desviación vertical disociada posterior a cirugía de endotropia no acomodativa appearance of dissociated vertical deviation after nonaccommodative endotropia surgery," *Revista Mexicana Oftalmol.*, vol. 78, no. 3, pp. 118–121, 2004.

[31] S. R. Hatt, X. Wang, and J. M. Holmes, "Interventions for dissociated vertical deviation," *Cochrane Database Syst. Rev.*, vol. 12, Nov. 2015, Art. no. CD010868.

[32] J. D. Mendola, I. P. Conner, A. Roy, S.-T. Chan, T. L. Schwartz, J. V. Odom, and K. K. Kwong, "Voxel-based analysis of MRI detects abnormal visual cortex in children and adults with amblyopia," *Hum. Brain Mapping*, vol. 25, no. 2, pp. 222–236, 2005.

[33] B. A. Fitzgerald and F. A. Billson, "Dissociated vertical deviation: Evidence of abnormal visual pathway projection," *Brit. J. Ophthalmol.*, vol. 68, no. 11, pp. 801–806, 1984.

[34] M. Gallegos-Duarte, G. Gonzalez-Perez, J. D. Mendiola-Santibanez, and D. Ibrahimi, "Study of visual pathway in strabismic children through tractography," *EC Ophthalmol.*, vol. 2, pp. 101–107, 2015.

[35] *CDC*. Accessed: May 20, 2020. [Online]. Available: https://www.cdc.gov/search/index.html

[36] R. W. Hertle, "A next step in naming and classification of eye movement disorders and strabismus," *J. Amer. Assoc. Pediatric Ophthalmol. Strabismus*, vol. 6, no. 4, pp. 201–202, Aug. 2002.

[37] K. Podoll and J. Lüning, "History of scientific research films in neurology in Germany 1895-1929," *Fortschritte Neurologie-Psychiatrie*, vol. 66, no. 3, pp. 122–132, 1998.

[38] A. Kawasaki, "Physiology, assessment, and disorders of the pupil," *Current Opinion Opthalmol.*, vol. 10, no. 6, pp. 394–400, Dec. 1999.

[39] N. J. Volpe, E. S. Plotkin, M. G. Maguire, R. Hariprasad, and S. L. Galetta, "Portable pupillography of the swinging flashlight test to detect afferent pupillary defects," *Ophthalmology*, vol. 107, no. 10, pp. 1913–1921, Oct. 2000.

[40] C. Hublin, E. Matikainen, and M. Partinen, "Autonomic nervous system function in narcolepsy," *J. Sleep Res.*, vol. 3, no. 3, pp. 131–137, Sep. 1994.

[41] F. E. Leon-Sarmiento, D. G. Prada, and C. E. Gutiérrez, "Pupila, pupilometría pupilografía," *Acta Neurol Colomb*, vol. 24, no. 4, pp. 188–197, 2008.

[42] E. Granholm, S. K. Morris, A. J. Sarkin, R. F. Asarnow, and D. V. Jeste, "Pupillary responses index overload of working memory resources in schizophrenia," *J. Abnormal Psychol.*, vol. 106, no. 3, p. 458, 1997.

[43] C. Girkin, "Evaluation of the pupillary light response as an objective measure of visual function," *Ophthalmol. Clinics North Amer.*, vol. 16, no. 2, pp. 143–153, Jun. 2003.

[44] R. P. Steck, M. Kong, K. L. McCray, V. Quan, and P. G. Davey, "Physiologic anisocoria under various lighting conditions," *Clin. Ophthalmol.*, vol. 12, p. 85, Oct. 2018.

[45] A. Rickmann, M. Waizel, S. Kazerounian, P. Szurman, H. Wilhelm, and K. T. Boden, "Digital pupillometry in normal subjects," *Neuro-Ophthalmol.*, vol. 41, no. 1, pp. 12–18, Jan. 2017.

[46] C. A. Schneider, W. S. Rasband, and K. W. Eliceiri, "NIH image to image J: 25 years of image analysis," *Nature methods*, vol. 9, no. 7, pp. 671–675, 2012.

[47] M. Hentschel and N. Page, "Selection of descriptors for particle shape characterization," *Properties Behav. Powders Other Disperse Syst.*, vol. 20, no. 1, pp. 25–38, 2003.

[48] M. D. C. Espino-Gudiño, "Morphological multiscale contrast approach for gray and color images consistent with human visual perception," *Opt. Eng.*, vol. 46, no. 6, Jun. 2007, Art. no. 067003.

[49] A. M. Herrera-Navarro, H. Jiménez-Hernández, H. Peregrina-Barreto, F. Manríquez-Guerrero, and I. R. Terol Villalobos, "Characterization of the roundness degree of graphite nodules in ductile iron: A new discrete measure independent to resolution," *Superficies y vacío*, vol. 26, no. 2, pp. 58–63, 2013.

[50] J. P. Bergmanso and J. G. Martinez, "Size does matter: What is the corneolimbal diameter?" *Clin. Experim. Optometry*, vol. 100, no. 5, pp. 522–528, 2017.

[51] M. C. Brodsky, "Dissociated horizontal deviation: Clinical spectrum, pathogenesis, evolutionary underpinnings, diagnosis, treatment, and potential role in the development of infantile esotropia (an American ophthalmological society thesis)," *Trans. Amer. Ophthalmol. Soc.*, vol. 105, p. 272, 2007.

[52] M. C. Brodsky, "Dissociated vertical divergence: Cortical or subcortical in origin?" *Strabismus*, vol. 19, no. 2, pp. 67–68, 2011.

[53] M. Gallegos-Duarte, "Paradoxical cortical response during the intermittent photo stimulation in the dissociated strabismus," *Cirugia Cirujanos*, vol. 73, no. 3, pp. 161–165, 2005.

[54] C. G. Cherfan, N. N. Diehl, and B. G. Mohney, "Prevalence of dissociated strabismus in children with ocular misalignment: A population-based study," *J. Amer. Assoc. Pediatric Ophthalmol. Strabismus*, vol. 18, no. 4, pp. 374–377, Aug. 2014.

[55] A. M. Khan, X. N. Li Ahmad, M. A. Korsten, and A. Rosman, "Chiropractic sympathectomy: Carotid artery dissection with oculosympathetic palsy after chiropractic manipulation of the neck," *Mount Sinai J. Med.*, vol. 72, no. 3, pp. 207–210, 2005.

[56] M. Dafereras, H. Sapouridis, K. Laios, D. Chrysikos, E. Mavrommatis, and T. Troupis, "The pioneer ophthalmologist johann friedrich horner (1831–1886) and the clinical anatomy of the homonymous syndrome," *Acta Chirurgica Belgica*, vol. 15, pp. 1–3, Apr. 2020.
[57] A. Invernizzi, P. Giardini, M. Cigada, F. Viola, and G. Staurenghi, "Three-dimensional Morphometric analysis of the iris by swept-source anterior segment optical coherence tomography in a Caucasian population," *Investigative Ophthalmol. Vis. Sci.*, vol. 56, no. 8, pp. 4796–4801, 2015.
[58] M. Brambilla, M. Biella, and M. E. Kret, "Looking into your eyes: Observed pupil size influences approach-avoidance responses," *Cognition Emotion*, vol. 33, no. 3, pp. 616–622, Apr. 2019.
[59] F. Manuri, A. Sanna, and C. P. Petrucci, "PDIF: Pupil detection after isolation and fitting," *IEEE Access*, vol. 8, pp. 30826–30837, 2020.
[60] Y. L. Yang, A. Fritz, L. Tor, and G. Per, "Methods to estimate areas and perimeters of blob-like objects: A comparison," in *Proc. IAPR*, Kawasaki, Japan, Dec. 1994, pp. 272–276.
[61] P. M. Swamidass, editor, *Mean Absolute Percentage Error (MAPE)*. Boston, MA, USA: Springer, 2004, p. 462.
[62] S. G. Rabinovich, *Measurement Errors and Uncertainties: Theory and Practice*. New York, NY, USA: Springer-Verlag, 2006.
[63] J. Silbert, N. Matta, J. Tian, E. Singman, and D. I. Silbert, "Pupil size and anisocoria in children measured by the plusoptiX photoscreener," *J. Amer. Assoc. Pediatric Ophthalmol. Strabismus*, vol. 17, no. 6, pp. 609–611, Dec. 2013.

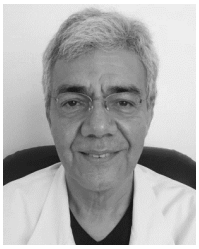

MARTÍN GALLEGOS-DUARTE received the Ph.D. degree in medical research from the University Autonomous of Querétaro, México (UAQ). He is currently an Ophthalmic Physician with UNAM, México. He is also a Professor/Researcher on the Bachelor of Optometry Faculty of Medicine (UAQ). His research interests include strabismus and neuroimage.

JORGE DOMINGO MENDIOLA-SANTIBAÑEZ (Member, IEEE) received the B.S. degree in electronics from the Benemérita Universidad Autónoma de Puebla, México, the M.S. degree in electronics from INAOE, México, and the Ph.D. degree from the Universidad Autónoma de Querétaro (UAQ), México. He is currently a Professor/Researcher with the UAQ. His research interests include mathematical morphology, medical imaging, and computer vision.

DANJELA IBRAHIMI received the master's degree in clinical optometry with the International Center of Optometry, Madrid, Spain, the Ph.D. degree in optometry with the International Center of Optometry, and Bircham University, Spain, the master's degree in medical research from the University Autonomous of Querétaro México (UAQ), and the Ph.D. degree from the Engineering Faculty, UAQ, México. Her research interests include brain stimulation through phototherapy, brain learning, and brain vision.

CARLOS PAREDES-ORTA was born in México, in 1983. He received the B.S. degree in computer systems engineer from the Technological Institute of Quéretaro (ITQ), and the M.S. and Ph.D. degrees in mechatronic engineering from the Center for Engineering and Industrial Development (CIDESI), in 2017. From 2017 to 2020, he was a Research with the Research Center in Research Optics (CIO). His research interests include mathematical morphology, medical imaging, and augmented reality.

JUVENAL RODRÍGUEZ-RESÉNDIZ (Senior Member, IEEE) received the M.S. and Ph.D. degrees in automation control from the University of Querétaro. Since 2004, he has been a part of the Mechatronics Department, UAQ, where he is currently working as a Researcher and Lecturer. His research interests include signal processing and motion control. He is the IEEE Vice-President of Querétaro State Branch. He received the award from the Mexican Academy of Sciences in 2016.

CARLOS ALBERTO GONZÁLEZ-GUTIÉRREZ received the M.S. and Ph. D. degrees in automatic control from the Universidad Autónoma de Querétaro (UAQ). He is currently a Professor with the Universidad del Valle de México, Campus Querétaro. His research interests include mechanisms and robot kinematics.